Experimental validation of a model for the transmission loss of a plate with an array of lumped masses

Carl Q. Howard (1) and Mike R.F. Kidner (1)

(1) School of Mechanical Engineering, The University of Adelaide, Adelaide, S.A. 5005, Australia

ABSTRACT

A theoretical model is developed to predict the transmission loss of a clamped rectangular plate with an array of lumped masses attached, and is compared with experimental measurements. An increase in the transmission loss of the plate was observed over approximately two octaves, in excess of that expected due to the effect of the 'smearing' the added mass over the plate, and these results compared well with a theoretical model. A laser vibrometer was used to measure the average velocity of the plate and the measured results compared favourably with theoretical predictions.

INTRODUCTION

The typical method of improving the low-frequency transmission loss through a finite plate is achieved by increasing the mass of plate. It is shown in this paper through experimental testing and a theoretical model, that it is possible to improve the transmission loss of a plate by attaching an array of masses to the plate, and the resulting transmission loss is greater than that which would be achieved by merely increasing the mass of the plate.

The placement of a rigid mass on plates has been considered by several researchers [Gardonio et al., 2001, Lunden and Kamph, 1982, Unruh, 1988, Kari, 2001, Vakakis, 1985, Gardonio and Elliott, 2000, Cutchins, 1980, St. Pierre Jr. and Koopman, 1995] to alter the vibration response of structures. The work presented here differs from many of the previously published research literature in that a large number of rigid masses attached to a plate has been considered, with the intention to improve the transmission loss of the plate, rather than reducing the vibration amplitude of the structure.

The following sections describe a mathematical model for the transmission loss of a finite plate with an array of rigid masses attached to the plate. Experiments were conducted to measure transmission loss of a rectangular clamped plate with and without an array of rigid masses and the results are compared with theoretical predictions.

MATHEMATICAL MODEL

Introduction

This section describes a mathematical model to predict the transmission loss of a clamped plate with rigid masses attached. The steps in the derivation of the mathematical model are divided into several sections, namely:

1. Calculation of the mode shapes of a clamped plate,
2. Calculation of the resonance frequencies of the clamped plate,
3. Equations of motion for a clamped plate that is driven by a general forcing function,
4. Couple the effects of rigid masses to the dynamics of the clamped plate,
5. Calculate the modal forcing function for an incident plane wave striking a simply supported plate, as shown in Figure 1 (a).
6. Use the modal forcing function in (5) to calculate the modal response of a *clamped plate*, in terms of the modal participation factors, as shown in Figure 1 (b).
7. Use the modal participation factors derived for the response of the clamped plate, to calculate the sound intensity radiated from a simply-supported plate of similar dimensions, as shown in Figure 1 (c).
8. Integrate the radiated intensity over an imaginary hemisphere to calculate the radiated sound power
9. Calculated the transmission coefficient for a plane wave striking a plate as the transmitted sound power divided by the incident sound power
10. Calculate the diffuse field transmission loss by integrating the transmission loss for plane wave transmission over all angles.

In the implementation of this method, steps (3) to (7) can be combined into one step.

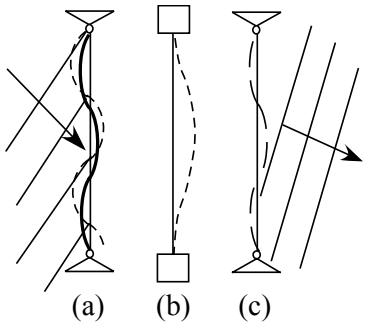

Figure 1: Schematic of the acoustic couplings between simply-supported and clamped plate models.

Mode Shapes

The mode shapes of a clamped plate are calculated by the multiplication of clamped beam modes (Warburton 1954). The procedure for calculating the mode shape functions involves calculating a pseudo- modal index k_m by calculating the roots of the equation

$$\cosh(k_m)\cos(k_m) - 1 = 0 \tag{1}$$

and has values listed in Table 1.

Table 1. Values of k_m

m	k_m
1	4.7300408
2	7.8532046
3	10.9956078
4	14.1371655
5	17.2787596
6	20.4203522
m>6	(2m+1) π/2

The displacement w of a clamped plate at position (x,y) can then be written as

$$w(x,y)=\sum_{m=1}^{\infty}\sum_{n=1}^{\infty}\psi_m(x)\psi_n(y)w_s \tag{2}$$

where w_s are the modal participation factors, and the mode shapes are defined as

$$\psi_m(x)=\left[\cosh\left(k_m x/L_x\right)-\cos\left(k_m x/L_x\right)\right] - D_m\left[\sinh\left(k_m x/L_x\right)-\sin\left(k_m x/L_x\right)\right] \tag{3}$$

$$\psi_n(y)=\left[\cosh\left(k_n y/L_y\right)-\cos\left(k_n y/L_y\right)\right] - D_n\left[\sinh\left(k_n y/L_y\right)-\sin\left(k_n y/L_y\right)\right] \tag{4}$$

where L_x, L_y are the lengths of the plate along the x and y axes, respectively,

$$D_m=\frac{\cosh(k_m)-\cos(k_m)}{\sinh(k_m)-\sin(k_m)} \tag{5}$$

and a similar equation can be written for D_n.

Resonance Frequencies

The resonance frequencies of a clamped rectangular plate can be calculated as (Leissa 1993)

$$\omega_{m,n}^2=A\left(G_m^4+G_n^4\left(\frac{L_x}{L_y}\right)^4+2\left(\frac{L_x}{L_y}\right)^2\left(\nu H_m H_n+(1-\nu)J_m J_n\right)\right) \tag{6}$$

$$A=\frac{E h^3}{12(1-\nu^2)}\times\frac{\pi^4}{L_x^4(\rho_p h)} \tag{7}$$

where E is the Young's modulus of the plate, h is the thickness, ρ_p is the density of the plate, υ is the Poisson's ratio, and the modal indicies $m,n=2\ldots\infty$ are defined using the convention described by Warburton (1954) where the index refers to the number of nodal lines, instead of the usual anti-nodal lines on the plate, and when m=2 or n=2, $G_2=1.506$, $H_2=J_2=1.248$, and for m>2 or n>2, $G_m=m-0.5$ $G_n=n-0.5$ and

$$H_m=J_m=(m-0.5)^2\times\left(1-\frac{2}{\pi(m-0.5)}\right) \tag{8}$$

with similar equations for H_n and J_n. After the calculation of the resonance frequencies of the clamped plate, the modal indicies m,n can be reduced by one to be consistent with the 'usual' definition for modal indicies that refers to the number of anti-nodes. The resonance frequencies and their indices can be sorted from lowest to highest frequencies, and the modal indices replaced by s.

Equations of Motion of the Plate

The equations of motion for the clamped plate that includes the inertial effects of the rigid blocks can be written as (Soedel, 1993)

$$\ddot{w}_s+2\xi_s\omega_s\dot{w}_s+\omega_s^2 w_s=\Gamma_s \tag{9}$$

where w_s is the s^{th} modal participation factor, ξ_s is the viscous damping coefficient of the shell at the s^{th} mode, ω_s is the resonance frequency of the s^{th} mode, and Γ_s is the s^{th} modal force which is applied to the shell for and is defined as

$$\Gamma_s=\frac{1}{\rho_p h N_s}\int_0^{L_x}\int_0^{L_y}\left[q_z U_{zs}+T_x U_{zs}+T_y U_{zs}\right]dy\,dx \tag{10}$$

where q_i and T_i represent the J^{th} point forces and point moments applied along each axis, which could be due to point forces or the point impedance due a lumped mass, and is defined as

$$q_{zJ}=F_{zJ}\,\delta(x-x_J)\delta(y-y_J)\,e^{j\omega t} \tag{11}$$

$$T_{iJ}=\frac{M_{iJ}}{R^2}\delta(x-x_J)\delta(y-y_J)\,e^{j\omega t} \tag{12}$$

where F_i and M_i are the forces and moments applied to the plate at location σ_J in the directions i = x,y,z , δ is the Dirac delta function, U_{is} is the modal response in the i^{th} direction, and for the vibrations of the plate considered here where only the out-of-plane transverse vibration is considered, the expressions can be written as

$$U_{xs}=0 \quad U_{ys}=0 \quad U_{zs}=[\psi]\mathbf{w}_p \tag{13}$$

$$N_s=\int_0^{L_x}\int_0^{L_y}U_{zs}^2\;dy\,dx \tag{14}$$

The force and moment loads on the plate are assumed to be point loads, which can be described with Dirac delta functions. Making use of the relationship

$$\int_{\alpha}F(\alpha)\frac{\partial}{\partial\alpha}\left[\delta\left(\alpha-\alpha^*\right)\right]d\alpha=-\frac{\partial F(\alpha^*)}{\partial\alpha} \tag{15}$$

the integral in Eq. (10) can be evaluated as

$$\Gamma_s=\frac{1}{\Lambda_s}\left[[\psi_J]^{\mathrm{T}}F_J-\frac{\partial[\psi_J]^{\mathrm{T}}}{\partial y}M_{Jx}+\frac{\partial[\psi_J]^{\mathrm{T}}}{\partial x}M_{Jy}\right] \tag{16}$$

where the modal mass is defined as $\Lambda_s=\rho h N_s$, which for a clamped plate is simply the total mass of the plate $\Lambda_p=\rho h L_x L_y$. The rotations of the plate are given by (Leissa, 1973, Soedel, 1993)

$$\theta_S=\frac{v}{R}-\frac{1}{R}\frac{\partial w}{\partial\theta} \tag{17}$$

$$\theta_\theta=-\frac{1}{R}\frac{\partial w}{\partial s} \tag{18}$$

$$\theta_w = \frac{1}{2R^2}\left(R\frac{\partial v}{\partial s} - R\frac{\partial u}{\partial \theta} \right) \tag{19}$$

The partial differentials of the mode shapes [ψ] with respect to the spatial co-ordinates in Eq. (16) are the mode shapes in the rotational directions. Hence Eq. (16) can be written as

$$\Gamma_s = \frac{1}{\Lambda_p}\left[[\psi_J]^{\mathrm{T}} F_J - [\psi_{J\theta x}]^{\mathrm{T}} M_{Jx} + [\psi_{J\theta y}]^{\mathrm{T}} M_{Jy} \right] \tag{20}$$

where $[\psi_{J\theta x}]$ and $[\psi_{J\theta y}]$ are the rotational mode shapes about the θ_x and θ_y axes, respectively and are

$$\frac{\partial \psi_m(x)}{\partial x} = \frac{k_m}{L_x}\left[\left(\sinh\left(k_m x / L_x\right) + \sin\left(k_m x / L_x\right) \right) - D_m\left(\cosh\left(k_m x / L_x\right) - \cos\left(k_m x / L_x\right) \right) \right] \tag{21}$$

$$\frac{\partial \psi_n(y)}{\partial y} = \frac{k_n}{L_y}\left[\left(\sinh\left(k_n y / L_y\right) + \sin\left(k_n y / L_y\right) \right) - D_n\left(\cosh\left(k_n y / L_y\right) - \cos\left(k_n y / L_y\right) \right) \right] \tag{22}$$

The impedance of the J^{th} mass attached to the plate is included as point translational and rotational inertias by using Eq (20) where

$$F_J = -\omega^2 m_J \tag{23}$$

$$M_{Jx} = -\omega^2 J_{Jx} \tag{24}$$

$$M_{Jy} = -\omega^2 J_{Jy} \tag{25}$$

where m_J is the mass of the block, J_{Jx} and J_{Jy} are the rotational inertias of the blocks along the x and y axes respectively.

As an example of the method in which the modal forcing function is calculated, consider a constant pressure load P applied to the plate the modal forcing function can be written as

$$\Gamma_s = \frac{P}{\rho h N_s}\int_0^{L_x}\int_0^{L_y} [U_{zs}]\, dy\, dx \tag{26}$$

For a clamped plate, Eq. (13) is substituted into Eq. (20) and hence the modal forcing function Γ_k is

$$\Gamma_{m,n} = \frac{P}{\rho h N_{m,n}}\left[\frac{2L_x}{k_m} \right]\left[\frac{\cosh(k_m) - \cos(k_m) - \sinh(k_m)\sin(k_m)}{\sinh(k_m) - \sin(k_m)} \right] \times \left[\frac{2L_y}{k_n} \right]\left[\frac{\cosh(k_n) - \cos(k_n) - \sinh(k_n)\sin(k_n)}{\sinh(k_n) - \sin(k_n)} \right] \tag{27}$$

The result in Eq. (27) is used to validate this model by comparing predictions of the displacement of the clamped plate subjected to a 1Pa loading with the results from predictions using a similar finite element model. The acoustic loading from an incident plane wave striking the plate is more complex than the result in Eq. (27) and is discussed in the following section.

Vibro-acoustic coupling of plate

Roussos (1985) describes a method to calculate the transmission loss of a simply-supported plate using modal summation techniques. This method was used in the vibro-acoustic model presented here to calculate the transmission loss of the clamped plate with masses attached. In summary, the method involves calculating the modal forcing function from an incident plane wave striking a simply-supported plate using the theory from Roussos (1985) (Step 5), using the modal forces to calculate the response of a clamped plate (Step 6), then using the response of the clamped plate to calculate the radiated sound pressure level from a simply-supported plate (Step 7), and finally using a Raleigh integral to calculate the sound power radiated from the plate (Step 8). Whilst this hybrid method is not precisely correct, as one should use the vibro-acoustic coupling for a clamped plate instead of a simply-supported plate as used here, it was found that, apart from significantly increasing the complexity of the mathematics, the TL predictions were reasonable estimates for the experimental measurements. The following paragraphs briefly describe the method used to calculate the modal forcing function. Further comments about the increase in complexity of the mathematics for the radiation from a clamped plate appear after the derivation for the radiation of a simply-supported plate.

The authors of this paper were unable to find suitable methods in the research literature for the calculation of the transmission loss of a rectangular plate with attached masses. However, some relevant previous studies have been conducted on transmission loss of rectangular plates; Sung and Jan (1997) considered the radiation from clamped plates, however they did not derive a closed-form solution to the problem based on the mode shapes of a clamped plate, and instead used an integration technique to calculate the over the plate. Similarly, Lomas and Hayek (1977), Berry et al (1990) also consider radiation from plates with general boundary conditions, but also did not derive the closed form solution. It would appear that most researchers utilise numerical integration techniques to solve this transmission loss problem, as closed-form solutions are unweildly. In the work presented here, numerical integration is conducted to calculate the acoustic power radiated from the plate.

The remainder of this section describes a mathematical model for the calculation of the transmission loss of a clamped rectangular plate, and can include the effects of masses attached to the plate.

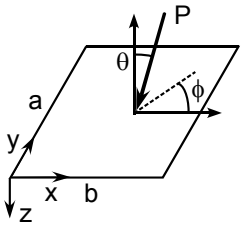

Figure 2: Coordinates for an incoming acoustic plane wave striking a rectangular plate.

Consider a plane wave of pressure P_i incident on a simply supported plate at angles θ and ϕ, as shown in Figure 2. The modal forcing vector can be written as (Roussos 1985)

$$p_{mn} = 8P_i\overline{Y}_m\overline{Y}_n \tag{28}$$

where

$$\bar{Y}_m = \begin{cases} \dfrac{-j}{2}\operatorname{sgn}(\sin\theta_i \cos\phi_i), \\ \text{where} \quad (m\pi)^2 = \left[\sin\theta_i \cos\phi_i (\omega L_x / c)\right]^2 \\ \dfrac{m\pi\left\{1-(-1)^m \exp\left[-j \sin\theta_i \cos\phi_i (\omega L_x / c)\right]\right\}}{(m\pi)^2 - \left[\sin\theta_i \cos\phi_i (\omega L_x / c)\right]^2} \\ \text{where} \quad (m\pi)^2 \neq \left[\sin\theta_i \cos\phi_i (\omega L_x / c)\right]^2 \end{cases} \tag{29}$$

$$\bar{Y}_n = \begin{cases} \dfrac{-j}{2}\operatorname{sgn}(\sin\theta_i \sin\phi_i), \\ \text{where} \quad (n\pi)^2 = \left[\sin\theta_i \sin\phi_i (\omega L_y / c)\right]^2 \\ \dfrac{n\pi\left\{1-(-1)^n \exp\left[-j \sin\theta_i \sin\phi_i (\omega L_y / c)\right]\right\}}{(n\pi)^2 - \left[\sin\theta_i \sin\phi_i (\omega L_y / c)\right]^2} \\ \text{where} \quad (n\pi)^2 \neq \left[\sin\theta_i \sin\phi_i (\omega L_y / c)\right]^2 \end{cases} \tag{30}$$

where c is the speed of sound in air. This modal force can be applied to the dynamics of the plate to calculate the modal participation factors, by substituting Eq. (28) into Eq. (20). It should be noted that similar equations could be derived for a clamped plate, however the authors were unable to find expressions in the research literature. The mode shape of a simply supported beam is characterised by a sine function, and the expression for the modal coupling is shown in Eq (29). For a clamped beam, there are four terms for the mode shape function, hence the acoustic modal coupling coefficient would comprise four terms, and for a clamped plate there would be eight terms for the modal coupling coefficient. Clearly, this would result in unwieldy equations. Once the modal participation factors are calculated, the transmited acoustic intensity can be calculated as

$$I_t = \frac{\rho_0}{2c}\left(\frac{4P_i L_x L_y}{\pi r \rho_p h}\right)^2 \left|\sum_{m=1}^{\infty}\sum_{n=1}^{\infty} Q_{mn}\right|^2 \tag{31}$$

where ρ_0 is the density of air,

$$Q_{mn} = \frac{Y_m Y_n \bar{Y}_m \bar{Y}_n}{(\omega_{mn}/\omega)^2 - 1 + 2j\xi\omega_{mn}/\omega} \tag{32}$$

$$Y_m = \begin{cases} \dfrac{-j}{2}\operatorname{sgn}(\sin\theta_t \cos\phi_t), \\ \text{where} \quad (m\pi)^2 = \left[\sin\theta_t \cos\phi_t (\omega L_x / c)\right]^2 \\ \dfrac{m\pi\left\{1-(-1)^m \exp\left[j \sin\theta_t \cos\phi_t (\omega L_x / c)\right]\right\}}{(m\pi)^2 - \left[\sin\theta_t \cos\phi_t (\omega L_x / c)\right]^2} \\ \text{where} \quad (m\pi)^2 \neq \left[\sin\theta_t \cos\phi_t (\omega L_x / c)\right]^2 \end{cases} \tag{33}$$

$$Y_n = \begin{cases} \dfrac{-j}{2}\operatorname{sgn}(\sin\theta_t \sin\phi_t), \\ \text{where} \quad (n\pi)^2 = \left[\sin\theta_t \sin\phi_t (\omega L_y / c)\right]^2 \\ \dfrac{n\pi\left\{1-(-1)^n \exp\left[j \sin\theta_t \sin\phi_t (\omega L_y / c)\right]\right\}}{(n\pi)^2 - \left[\sin\theta_t \sin\phi_t (\omega L_y / c)\right]^2} \\ \text{where} \quad (n\pi)^2 \neq \left[\sin\theta_t \sin\phi_t (\omega L_y / c)\right]^2 \end{cases} \tag{34}$$

and $\xi = C_D/(2\rho_p h \omega_{mn})$. The transmitted power Π_t can be calculated by integrating the transmitted intensity I_t over a far-field hemisphere such that

$$\Pi_t = \int_{\phi_t=0}^{2\pi}\int_{\theta_t=0}^{\pi/2} I_t r^2 \sin\theta_t \, d\theta d\phi \tag{35}$$

Equation (35) is evaluated numerically in the work presented here. Finally, the transmission loss TL is calculated as

$$TL = 10\log_{10}\left(\Pi_i / \Pi_t\right) \tag{36}$$

and the incident acoustic power Π_i is given by

$$\Pi_i = \left(P_i^2 L_x L_y \cos\theta_i\right)/(2\rho_0 c) \tag{37}$$

The sound field inside the reverberation chambed used in the experimental part of the work conducted here is assumed to be a diffuse acoustic field. A diffuse acoustic field is characterised by an infinite number of uncorrelated plane-waves. Suppose that one is interested in the diffuse field quadratic response of a physical quantity denoted as $Q(\theta,\phi)$. One can show that the quadratic response Z^2 is given by (Nelisse et al 1996)

$$Z^2 = \int_0^{\pi}\int_0^{2\pi} \sin\theta \left|Q(\theta,\phi)\right|^2 d\phi \, d\theta \tag{38}$$

For each orientation (θ,ϕ) of plane waves striking the plate, the transmission loss of the system must be calculated. A total of 370 plane-waves (i.e. 10 degree increments) were used here to simulate the diffuse field in the analysis presented here. Nelisse et al (1996) used 324 plane-waves to simulate a diffuse field and found that using more plane-waves does not affect significantly the diffuse field response.

The calculation of the transmission loss of the plate at 100 discrete frequencies for a plane wave took approximately 3 minutes on a 3GHz desktop, using a Matlab program. The calculation of the transmission loss for 370 plane waves would take approximately 18.5 hours. Instead of using a single desktop for the calculations, a distributed computing network was used which is described in Howard et. al. (2005). Each of the 370 calculations for the transmission loss of the plane waves from a particular angle of incidence was submitted to one computer on a distributed computing network, which reduced significantly the calculation time.

EXPERIMENT

The transmission loss of a clamped aluminium plate was experimentally measured. The plate had the properties described in Table 1.

Table 1. Geometry of the plate

Width L_x	1.0	m
Height L_y	1.5	m
Thickness t	0.0015	m
Density ρ	2700	kg/m^3
Young's Modulus E	70	GPa
Poisson's ratio ν	0.33	No units
Loss factor η	0.01	No units

Figure 3 (a) shows a picture of the aluminium plate with an array of 49 rigid masses attached to it. Figure 3 (b) shows a close-up of the rigid masses. Figure 4 shows a picture of the laser vibrometer that was used to measure the vibration response of the plate due to the acoustic excitation.

Figure 5 shows the measured weights of the rigid masses that were attached to the plate. Figure 6 shows the location of where each mass was placed on the plate – the top left corner

of the plate had the lightest mass (block 1), and the bottom right corner had the highest mass (block 49). No attempt was made to optimise the location of the rigid masses in this work. The optimisation of the locations of the rigid masses is the subject of future work. The purpose of the work conducted here is to develop a mathematical model for the transmission loss of the plate with the array of masses, which could be used with a genetic algorithm to determine optimal locations.

The mathematical model of the vibration response of the plate was first compared with a finite element model of the plate modelled in ANSYS. Figure 7 shows the displacement at centre of plate due to 1Pa pressure applied to the plate. The results show that the modal model of the plate compares favourably with the ANSYS predictions. Another verfication was done to ensure the coupled response of the plate and rigid masses was correct, however the results are not presented here. Hence the results provide confidence that the dynamics of the clamped plate have been modelled correctly.

Figure 8 shows the experimentally measured transmission loss of the plate with and without the rigid masses attached. The solid curve shows the predicted transmission loss for a finite plate based on the work by Sewell (1970), and discussed in Fahy (1994, p162). The dashed line shows the predicted response for an infinite plate (Beranek and Ver 1992, p286). The curve with the crosses (x) shows the experimentally measured transmission loss for the bare plate and compares favourably with the predictions for the finite plate between 100-8000Hz. The reverberation chambers used for the tests only provide valid results above about 100Hz and is a function of the largest dimension of the chambers. It can be seen that the measured TL above 10kHz does not follow the theoretical predictions. The experimental measurements of the T60 reverberation times above 10kHz were erroneous, and were caused by insufficient sound level in the receiver room above the background level for the measurement of the 60dB change in sound levels and an insufficient number of spectral samples during the decay measurements, and hence the predicted TL values are inaccurate. Figure 9 presents the same results as Figure 8 only the frequency scale has been reduced to 100-1000Hz, to highlight the results. The figure shows that the plate with the array of masses improved the transmission loss of the plate by upto 5dB over the frequency range from 150-400Hz. This figure also shows the theoretically predicted transmission loss for a finite plate based on Sewell's theory, for a plate of equivalent thickness (1.79mm) if the mass from the blocks (1.177kg) had been smeared across the plate. The TL is about 1.2dB greater than the standard thickness plate. Hence, the results show that the effect of the array of masses significantly improved the transmission loss of the plate, greater than the benefit that could be achieved by simply 'smearing' the mass.

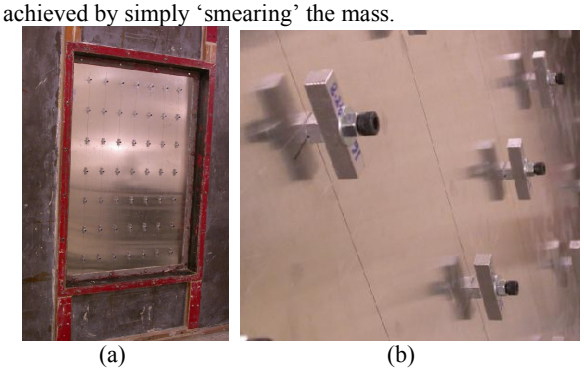

(a) (b)

Figure 3: (a) pictures of the clamped plate in the transmission loss test facility, (b) close-up of the rigid blocks attached to the plate.

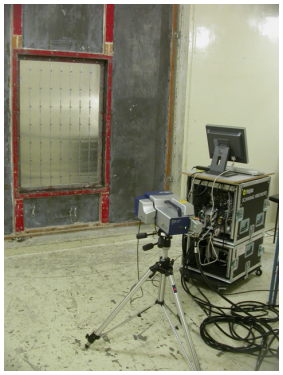

Figure 4: Picture inside the source room of the transmission loss test facility, showing the laser vibrometer.

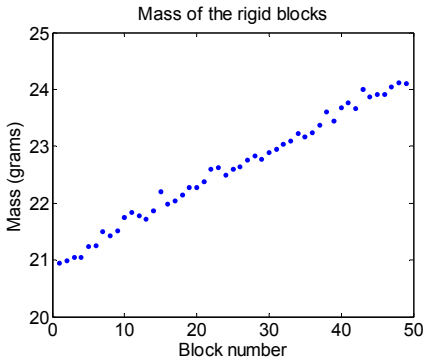

Figure 5: Weights of the 49 rigid blocks.

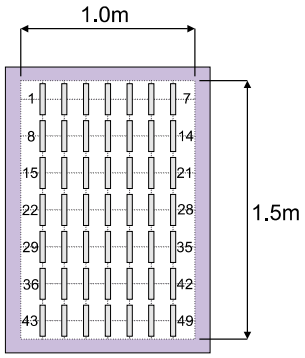

Figure 6: Locations of the 49 rigid blocks on the plate.

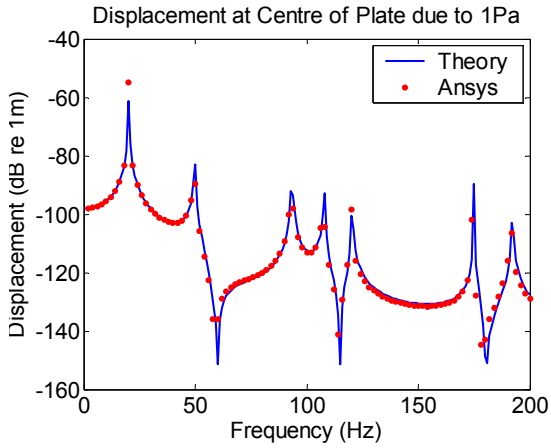

Figure 7: ANSYS and theoretical prediction of the displacement at the centre of a clamped plate due to a 1Pa loading.

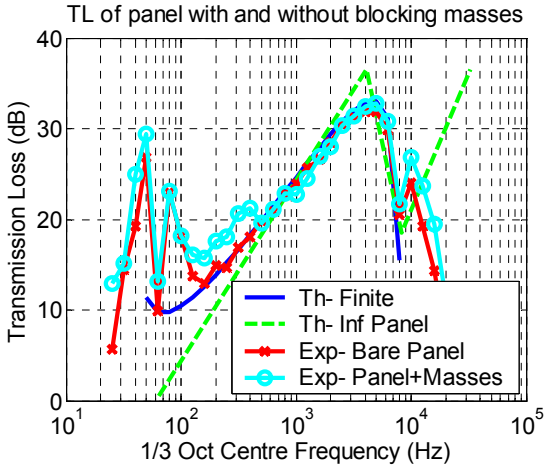

Figure 8: Experimentally measured and theoretically predicted transmission loss of a clamped plate with and without an array of rigid masses.

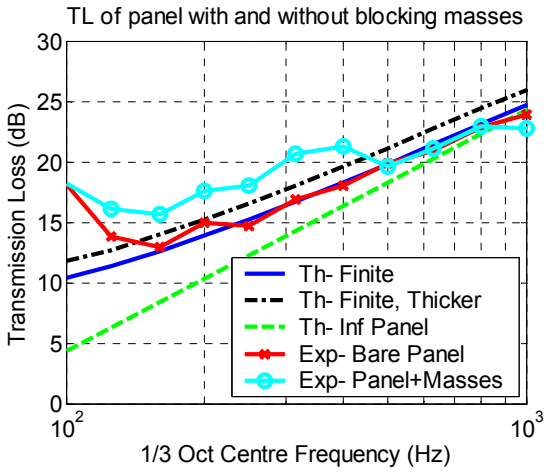

Figure 9: Results from Figure 8 from 100 to 1000Hz.

The transmission loss of a plate depends on the acoustic field that strikes the plate. Figure 10 shows the predicted transmission loss for an infinite plate of 1.5mm thick, when subjected to normal incidence, field incidence and diffuse field acoustic conditions, which were calculated using the theories from Fahy (1994, p158), and the experimentally measured transmission loss the plate without masses attached. The theoretical results show that one can expect a variation in the quoted TL values, depending on the type of acoustic field that strikes the plate. It has been assumed that the experimental testing in the reverberation chambers approximates *field incidence* conditions, whereas, the results from the theoretical predictions presented here are for *diffuse field* conditions. Hence, when comparing the experimental and theoretical results, one should be mindful that due to the different acoustic loading conditions, one should expect differences in the results.

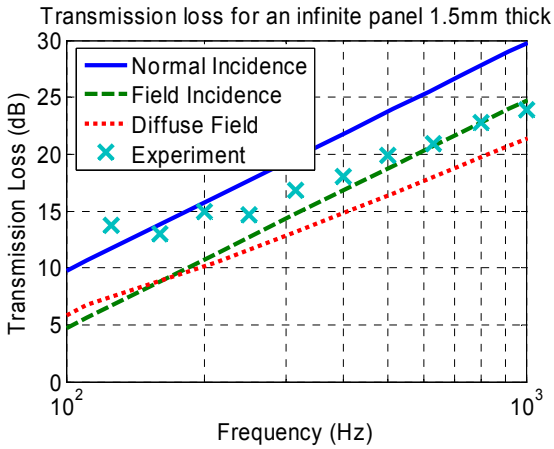

Figure 10: Theoretical TL of infinite plates for three types of acoustic fields.

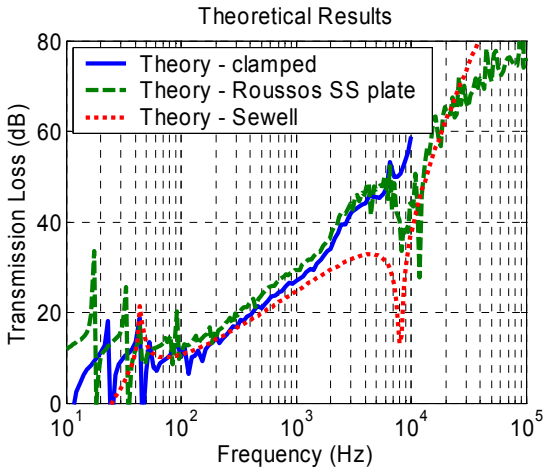

Figure 11: Comparison of Roussos' simply-supported plate model, the clamped plate model, and Sewell.

Figure 11 shows the comparison of the Roussos model for the TL of a simply-supported rectangular plate for a single plane wave at incidence normal to the panel, with the dimensions of the plate considered here, the predicted TL using the theoretical model presented here for the clamped-plate, and the theoretical model by Sewell for a finite plate. The results show that there is good agreement for the predictions of the simply-supported and the clamped plate models in the frequency range from 100 to 5000Hz, which covers the range of interest. Greater accuracy can be achieved at frequencies > 5000Hz if more plate modes are included in the analysis, but is not required for the purposes of the current work.

Figure 12 shows the experimentally measured TL of the bare plate for *field incidence* acoustic loads, the TL for a finite plate using the theory from Sewell, and the TL for a finite plate in a *diffuse field* using the theory described here. The results show that the experimental results are very similar to the Sewell's predictions for a finite plate. The predictions for the TL of the clamped plate using the theory described here is about 8dB lower than the experimentally measured results. One would expect a difference in field incidence and diffuse field results of around 5dB at 1000Hz, as shown in Figure 10, however the difference in the acoustic fields at low frequencies (100Hz) is negligible.

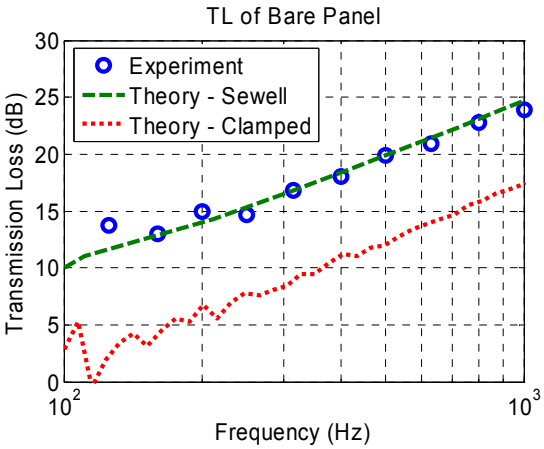

Figure 12: TL of bare plate.

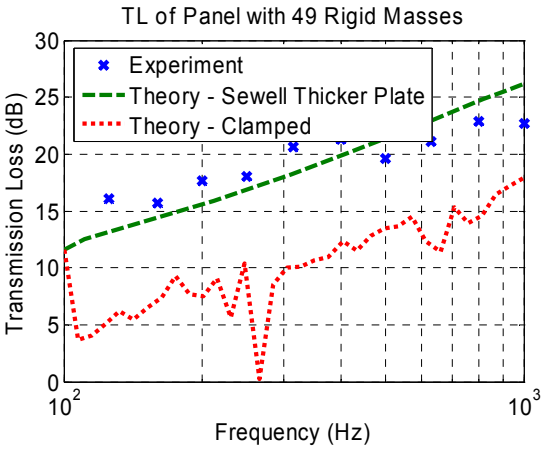

Figure 13: TL of plate with 49 masses attached.

Comparison of the predictions for the clamped plate theory in Figure 11 for a single plane wave, and Figure 12 for a *diffuse field*, shows that the TL decreases by about 8dB. The TL for a *diffuse field* is calculated using Eq. (38) and it is this integration of the TL results for the plane wave that causes the reduction in the TL.

Figure 13 shows the experimentally measured TL of the plate with 49 masses attached for *field incidence* acoustic loads, the TL for a finite plate that has the equivalent thickness that corresponds to the weight of the masses smeared across the plate using the theory from Sewell, and the TL of the plate using the clamped plate model presented here. The experimentally measured results show that the improvement in the TL due to the masses exceeds the benefit of just increasing the thickness of the plate. The theoretical predictions using the model presented here are about 10dB lower than the experimentally measured TL. As described above, some of the discrepancy can be attributed to the different acoustic loading conditions.

Figure 14 shows the comparison of the experimentally measured and theoretically predicted TL of the plate with and without the masses attached. The experimental results show that there is an improvement in the TL of about 3dB over the frequency range from 125-400Hz. The absolute levels of the predicted transmission loss using the theory described are lower than the experimentally measured results. However, the important result is that the theoretical model shows that there is an improvement in the TL over a frequency range due to the addition of the masses, which is the same qualitative result that can be seen in the experimental results.

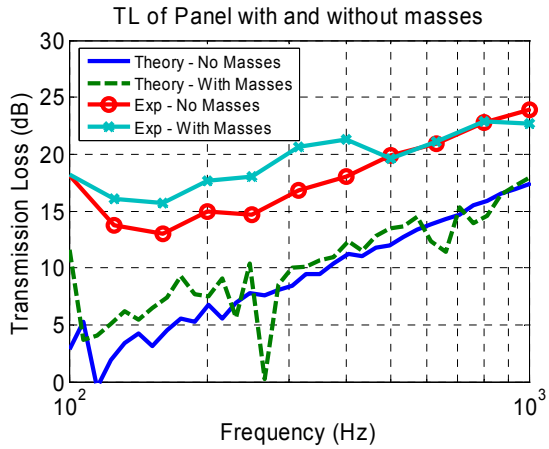

Figure 14: TL of plate for theoretical and experimental results.

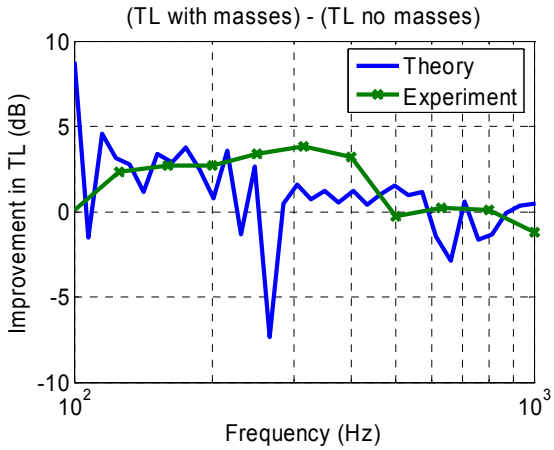

Figure 15: Improvement in TL due to the addition of rigid masses.

Figure 15 shows that improvement in the TL, which is calculated as the TL with the masses attached to the plate minus the TL without the masses attached to the plate, for the theoretical predictions and the experimental results. The results show that the predicted benefit due to the addition of the masses is similar to the experimentally measured benefit.

Figure 16 shows the experimentally measured average squared velocity of the plate with and without the masses attached. The velocity of the plate was measured using the laser vibrometer at 191 points. The results show that there is a general decrease in the velocity in the frequency range from 100-200Hz. Note that the velocity measurements were normalised with the voltage that was supplied to the power amplifiers in the source chamber, hence the absolute values of the average squared velocity are not meaningful.

Figure 17 shows the corresponding theoretically predicted average squared velocity of the plate, which is calculated by squaring the modal participation factors of the plate and multiplying by the square of the frequency (i.e. $\omega^2[w_s]^H[w_s]$). The velocity results are normalised for a 1Pa incident pressure. The results show that the masses alter the vibration response of the plate, but the mechanism that caused the improvement in the transmission loss due to the addition of the rigid masses requires further investigation. It is possible that the effect of the rigid masses is to 'pin' locations on the plate, thereby changing the mode shapes of the plate.

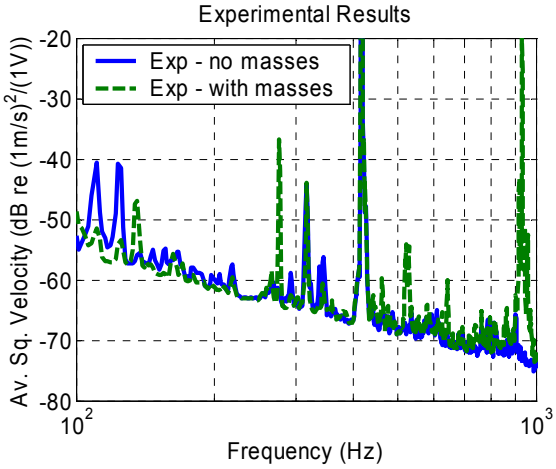

Figure 16: Experimentally measured average square velocity of the plate.

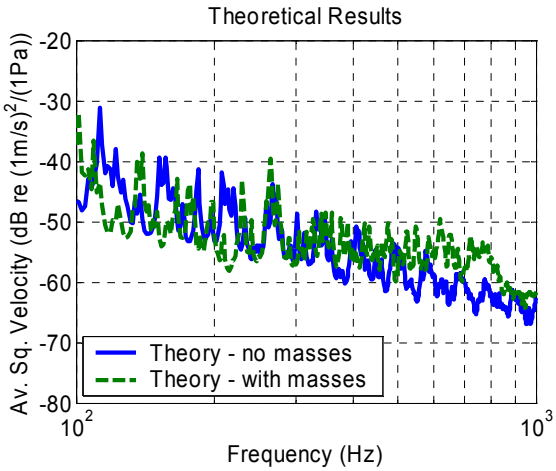

Figure 17: Theoretically predicted average squared velocity of the plate.

The theoretical results do not match the results from the experimental testing. There are several reasons that might explain the discrepancies. The damping coefficient used in the theoretical models was 1%, which was not verified and it is possible that it could be greater. The theoretical model has provisions for the inclusion of the effects of the rotational inertia of the masses, but was not included in the predictions presented here. It is hypothesised from previous work (Howard et. al. 2005) that the rotational inertia from masses can be important and can lead to greater vibration reduction that if rotational inertia had not be included. The most likely cause for the discrepancies is the method by which the diffuse field was simulated and whether this method is representative of the acoustic testing conditions in the reverberation chamber. The theoretical model used to predict the TL through a simply-supported plate for a single plane-wave was based on Roussos' (1985) model. The predictions presented in Roussos' paper, and those presented here for a simply-supported plate are similar to Sewell's predictions for a *diffuse field*. However, as shown in Figure 10, one would expect that the TL predictions for *plane-waves* (normal incidence) should be greater than that for *diffuse field* conditions. Hence, it is possible that Roussos' model might under-predict the TL for a plane-wave, and hence the predicted TL for *diffuse field* conditions is also under-predicted.

CONCLUSIONS

A theoretical model was developed to enable the prediction of the transmission loss of a clamped plate with rigid masses attached and was compared with the results from experimental testing. In qualitative terms the results showed that the masses improved the TL of the plate greater than that which would have been achieved if the added mass had been 'smeared' across the plate. The experimental results showed improvement in the TL of about 3dB in the frequency range from 100 to 400Hz – almost two octaves, and the qualitative results from the simulations also indicated improvement in the TL over a similar frequency range. The magnitudes of the predicted TLs between the theoretical predictions and the experimental results differed, which could be attributed to the differences in the assume incident acoustic field striking the plate, and also the coefficient of damping used in the model.

The model presented here will be used in the future to determine the optimum locations the rigid masses that will maximise the transmission loss of the plate.

ACKNOWLEDGEMENTS

The authors gratefully acknowledge the financial support of Australian Research Council for the purchase of the laser vibrometer used in the experimental part of this work.

REFERENCES

Beranek, L.L. and Ver, I.L., 1992, Noise and vibration control engineering, principles and applications, John Wiley & Sons.

Berry, A. Guyader, J-L, Nicolas, J, 1990, A general formulation for the sound radiation from rectangular baffled plates with arbitrary boundary conditions, Journal of the Acoustical Society of America, 88 (6), December, p2792-2802.

Cutchins, M. A., 1980, The effect of an arbitrarily located mass on the longitudinal vibrations of a bar. Journal of Sound and Vibration, 73 (2):185–193, 1980.

Fahy, F., 1994, Sound and Structural Vibration, Radiation, Transmission and Response, Academic Press, London.

Gardonio, P. and Elliott, S.J., 2000, Passive and active isolation of structural vibration transmission between two plates connected by a set of mounts. Journal of Sound and Vibration, 237(3):483–511.

Gardonio, P., Ferguson, N.S., and Fahy, F.J., 2001, A modal expansion analysis of noise transmission through circular cylindrical sell structures with blocking masses. Journal of Sound and Vibration, 244(2):259–297, 5 July.

Howard, C.Q. and Hansen, C.H., and Zander, A.C. 2005, Optimisation of Design and Location of Acoustic and Vibration Absorbers Using a Distributed Computing Network, Proceedings of Acoustics 2005, Busselton, Western Australia, Australia, 9-11 November, p173-178.

L. Kari. Dynamic transfer stiffness measurements of vibration isolators in the audible frequency range. Noise Control Engineering Journal, 49(2):88–102, March-April 2001.

Lomas, N.S., and Hayek, S.I., 1977, Vibration and acoustic radiation of elastically supported rectangular plates, Journal of Sound and Vibration, 52 (1), p1-25.

Lunden, R. and Kamph, E., 1982, Vibration isolation of a damped skeletal machine foundation - theory and experiment. Journal of the Acoustical Society of America, 71(3):600–607, March.

Nelisse, H., Beslin, O., and Nicolas, J., 1996, Fluid-structure coupling for an unbaffled elastic panel immersed in a diffuse field, Journal of Sound and Vibration, 198 (4), p485-506.

St. Pierre Jr., R.L. and Koopman, G.H., 1995, Design method for minimizing the sound power radiated from plates by adding optimally sized, discrete masses. Transactions of the ASME, Journal of Mechanical Design, 117B:243–251.

Roussos, L.A., 1985, Noise transmission loss of a rectangular plate in an infinite baffle, NASA technical paper TP2398, March, Langley Research Center, Hampton, Virginia, USA.

Soedel, W., 1993, Vibrations of Shells and Plates, Marcel Dekker.

Sewell, E.C., 1970, Transmission of reverberant sound through a single-leaf partition surrounded by an infinite rigid baffle, Journal of Sound and Vibration, 12 (1), p21-32.

Sung, C-C and Jan, C.T, 1997, Active control of structurally radiated sound from plates, Journal of the Acoustical Society of America, 102 (1), July, p370-381.

Unruh, J.F., 1988, Structure-borne noise control for propeller aircraft. Journal of Aircraft, 25(8).

Vakakis, A.F., 1985, Dynamic analysis of a unidirectional periodic isolator, consisting of identical masses and intermediate distributed resilient blocks, Journal of Sound and Vibration, 103(1):25–33.

Wallace, C.E., 1972, Radiation resistance of a rectangular panel, The Journal of the Acoustical Society of America, 51 (3) part 2, p946-952.

Warburton, G.B, 1954, The Vibration of rectangular plates, Proceedings of the Institute of Mechanical Engineers, 168, p371-384.